HARVARD COASTAL/DEEP WATER PRIMITIVE EQUATION MODEL

Carlos J. Lozano, Patrick Haley, Hernan Arango, Quinn Sloan and Allan R. Robinson

July 7, 1994

Introduction

The Harvard Dynamical Modelling System consists of a Primitive Equation model (Spall & Robinson 1989), a Quasi-Geostrophic model (Miller et. al. 1983, Milliff 1990 and Özsoy et. al. 1992) and a Surface Boundary Layer model (Walstad & Robinson 1993). The emphasis here is place on the Harvard Primitive Equation Model for Coastal and Deep Water. This model is applicable to any oceanic region, with arbitrary coastline and/or open boundary segments. The basic dynamical integration algorithm is that of the GFDL model. The deep ocean version of the Harvard model was developed by adding open boundary conditions, terrain following coordinates, and subgrid scale physics appropriate for mesoscale resolution. The following features were included:

- Terrain following coordinate system in the vertical with flat upper levels in order to support higher accuracy in the upper ocean and the main thermocline.
- Open boundary conditions using a Charney-Friedrichs-VonNeumann condition for the local vorticity (internal and external components) in the absence of forcing terms.
- Shapiro filter parameterization of horizontal or isopycnal subgrid diffusivities.
- Rotatable domains for various orientations of regional models.

Further extensions have been carried out for accurate computations in the deep ocean with steep topography, the shelf break and the shelf region. The new model features, of particular interest for the work in this project, include:

- The terrain following coordinate systems include a double σ vertical coordinate system allowing a smooth transition from the coast to the deep sea.
- Algorithms for accurate computation of the pressure gradient over steep and tall topography.
- Algorithms for accurate computation of horizontal and vertical stresses and tracer dissipative fluxes in sigma coordinates.
- Algorithms to smooth and condition the topography with minimal distortion.
- The introduction of coasts and islands in an otherwise open domain.
- The option to use either a rigid lid or a free surface.

- The Large and McWilliams (1994) parameterization of vertical processes.
- The bottom boundary layer parameterization of Grant and Madsen (1982).

The GFDL algorithms are documented in Bryan (1969) and Cox (1984). The details of the deep ocean model developments are expounded in Spall (1988) and Spall and Robinson (1989). In what follows, a somewhat self contained description of recent developments is given. These and future developments are facilitated by modular codes managed under the UNIX source control system and code pre-processing options that allow the flexible support of diverse hardware platforms, physics and algorithm options.

Model Physics

The Primitive Equation Model is based upon the Navier-Stokes equation in a rotating reference frame with the following two main simplifying assumptions, appropriate for most of the deep ocean and shelf regions. The first is the Boussinesq approximation, which retains density variations only in the buoyancy terms. The second is the hydrostatic approximation. The canonical primitive equations include further approximations based on dimensional analysis. In particular, the geopotentials are assumed to lie on concentric spheres; the gravitational field is taken to be constant throughout the domain; only the vertical component of the Earth rotation vector is retained; the solid boundaries are assumed to be rigid and impermeable and the heat and salt fluxes normal to the solid boundaries are assumed to be null. A free surface option will be available in the near future.

Under these assumptions the canonical primitive equations are (Pedlosky, 1987):

$$\nabla \cdot \vec{u} + \frac{\partial w}{\partial z} = 0$$

$$\frac{\delta \vec{u}}{\delta t} + f\vec{e}_z \times \vec{u} = -\nabla p + Div\ \tau + \vec{F}_m$$

$$\frac{\partial p}{\partial z} = -g\rho$$

$$\frac{\delta T}{\delta t} = Div\ \vec{q}_T + F_T$$

$$\frac{\delta S}{\delta t} = Div\ \vec{q}_S + F_S$$

$$\rho = \rho(T, S, p)$$

where $\boldsymbol{Div}$ is the three dimensional divergence operator; $\nabla\cdot$ is the horizontal divergence operator; ∇ is the horizontal gradient; $\vec{e}_z$ is a unit vector in the vertical direction; $\delta/\delta t$ is the material derivative; $\vec{u}, w$ the horizontal and vertical velocities; p is the pressure; ρ is the density; f is the Coriolis parameter; τ is the stress tensor; $\vec{F}_m$, F_T and F_S are the chosen parameterizations for additional subgrid scale physics and $\vec{q}_T$, $\vec{q}_S$ are the heat and salinity flux vectors.

Coordinate systems

The realization of these equations in spherical coordinates is standard, e.g. Bryan (1969); but it should be noted that in most numerical models, including the GFDL model and ours, some of the metric terms are not included, since scaling arguments suggest that they are negligible. A sigma coordinate system retains the angular coordinates of the spherical coordinate system and replaces the radial coordinate z by

$$\sigma = F(z, h)$$

where the mean surface of the ocean is set at $z = 0$, the bottom of the ocean is at $z = -h$, and the function F is strictly increasing with $F(0, h) = 1$ and $F(-h, h) = -1$. In practice, the numerical model implements either a linear sigma coordinate system

$$F = 1 + 2z/h$$

or piecewise linear sigma. For the latter, the simplest one, known as the hybrid system (Simmons and Burridge,1981), is given by

$$F = 1 + z/h_c \text{ for } 0 > z > -hc$$

$$F = (z + hc)/(h - hc) \text{ for } -hc > z > -h$$

where h_c is a constant. The constant h_c must be positive and bounded away from the minimum of h. In order to maintain relatively flat levels in the deep ocean, another piecewise linear system is obtained by replacing in the constant h_c by a function that allows a suitable transition of the level $\sigma = 0$ from the shelf to the open ocean while maintaining approximately flat levels for $\sigma > 0$. This coordinate system is called the double sigma system. Figure 1 illustrates some of the properties of the double sigma coordinate system.

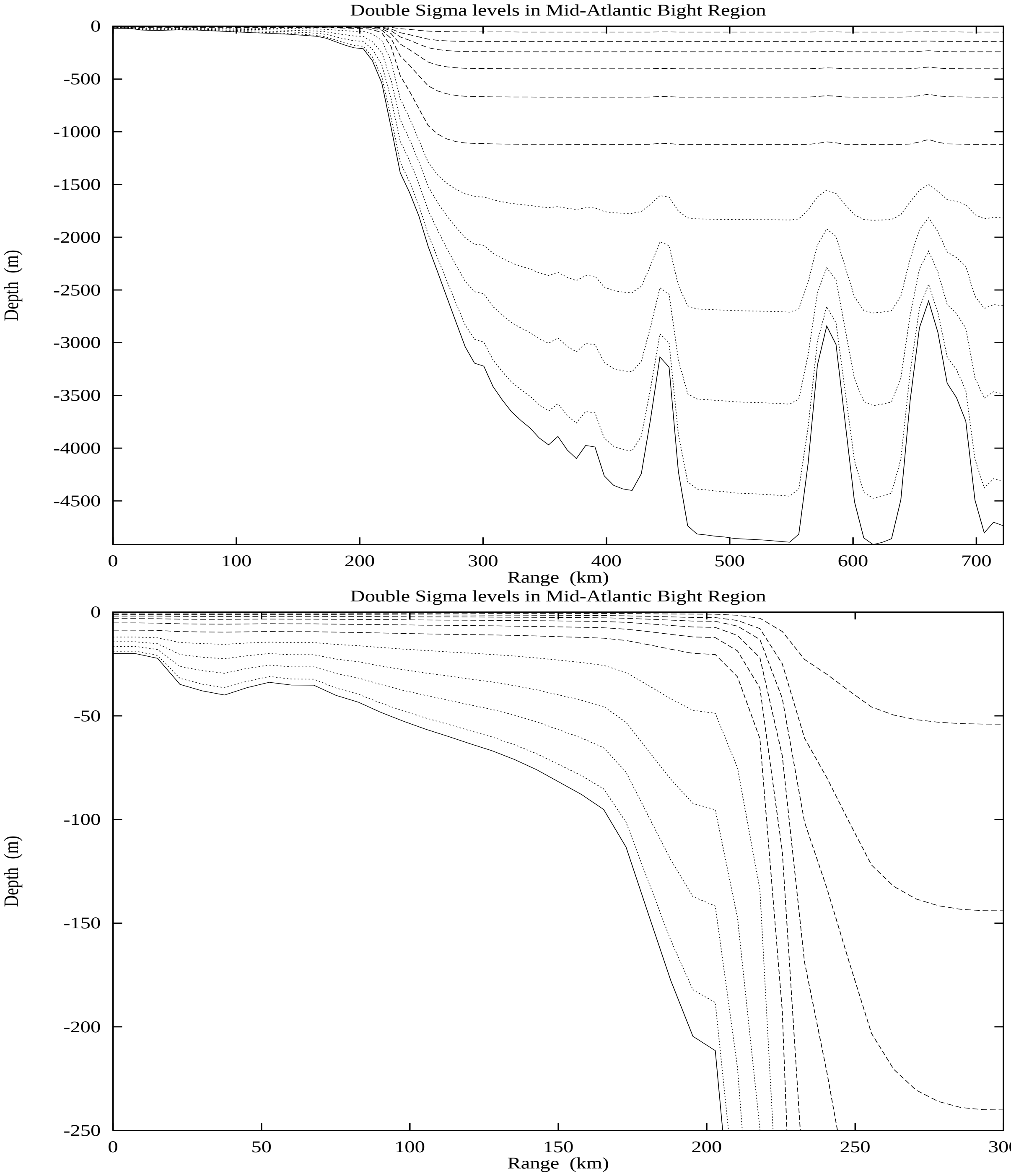

Figure 1. An examination of the double σ-system in the Mid-Atlantic Bight region. Displayed on top are the levels throughout the entire water column, beneath is a blow up of the upper 250 meters. Notice that the upper levels remain flat over the seamounts while a good resolution is maintained over the shelf, slope and basin regions. The interface function, $h_c(x,y)$, for the double σ-system is given by $h_c(x,y) = \frac{z_{c_2}+z_{c_1}}{2} + \frac{z_{c_2}-z_{c_1}}{2} \cdot \tanh\left\{\frac{2\alpha}{z_{c_2}-z_{c_1}}\left[h(x,y) - h_{ref}\right]\right\}$ where $z_{c_1} = -10$ (m), $z_{c_2} = 1500$ (m), $h_{ref} = 1000$ (m) and $\alpha = 1$.

Standard derivations of the primitive equations for this class of non-orthogonal coordinate systems start from the equations in spherical coordinates, see e.g. Bleck (1978), instead of a coordinate free form. As a consequence, some of the additional metric terms, for instance those related to the theory of parallel translation in differential geometry, are necessarily overlooked. A coordinate free derivation indicates that the omitted terms are negligible if $\nabla h << 1$. Since this inequality holds for most oceanic conditions, we will use arguments depending upon the direct transformations from the spherical to the sigma coordinate system. Finally, we use freely, whenever it is convenient in the arguments and in the model, the beta plane approximation (LeBlond and Mysak, 1978)

Horizontal Gradients and the Hydrostatic Consistency Condition

The transformation from z to σ coordinates of the horizontal gradient of G is

$$(\nabla G)_z = (\nabla G)_\sigma - \frac{\partial G}{\partial \sigma}(\nabla \sigma)_z$$

where the subscripts indicate the variable that is held constant on the derivation. The right hand side is now amenable to a finite difference discretization in terms of quantities defined over the σ-grid. Haney's (1990) analysis of the truncation errors shows that for a second order difference approximation to the right hand side, it is necessary that in the present notation and for linear sigma coordinates,

$$HCF \equiv \left[\frac{1-\sigma}{2\delta\sigma}\right] \frac{1}{h} \left|\frac{\partial h}{\partial x}\right| \delta x < 1 \; .$$

A similar inequality holds for the y-derivatives. In the above equation σ is taken at the z-surface where the horizontal gradient is required, $\delta\sigma$ is the thickness of the σ-layer and δx is the horizontal grid spacing. Near the upper bound 1, the results are disastrous and a conservative bound of 1/2 is more appropriate.

These inequalities are dubbed the hydrostatic consistency condition. The name seems to be derived from the fact that the analysis was carried out for the pressure gradient term; but naturally it will hold for all the horizontal gradient terms. For instance, the lateral heat flux is usually parameterized, as we do in our model, in the form

$$\vec{q}_H = K_H (\nabla_H)_z T \; ;$$

and the above inequality is required if the discretization suggested by the chain rule is followed.

The method selected to compute the horizontal gradients is to interpolate, in the vertical, the values at the z-surfaces. In this fashion, standard second order and fourth order (McCalpin, 1994) finite differences for the horizontal gradients are computed. The estimate of the truncation errors are the summation of the truncation errors due to the horizontal differences plus the truncation errors due to the differencing of the interpolation errors. A crude estimate for the latter yields the same truncation errors as the interpolation, if the cross derivatives associated with the bound for the interpolation and the finite differences are sufficiently small. In practice, this requires a careful control on the smoothness of the fields.

At a given computational box, if the collocation of values at a z-surface can be performed by interpolation then the error bound of the consistency condition does not apply. Alternatively, if the collocation of a value at a z-surface requires an extrapolation, then the error of the extrapolation error is proportional to a power of $\delta h/\delta z$ where δz is the thickness of the box and δh is the typical change in depth of the edges of the box. For the linear sigma system, $HCF = \delta h/\delta z$; thus, in practice, the extrapolation errors can be improved independently by reducing the horizontal grid spacing, by judiciously selecting the σ-levels (first term in brackets), or by an appropriate change of the topography h.

The pressure gradient computation requires the integration of the hydrostatic equation, namely

$$p(z) = -g \int_z^0 \rho(s) ds \ .$$

The interpolating polynomial is integrated and, in the actual computations, roundoff error growth is avoided by computing the integral from level k to level $k+1$ using

$$\frac{\delta p(z_{k+1})}{\delta x} = \frac{\delta p(z_k)}{\delta x} + \int_{z_k}^{z_k+1} g \frac{\delta[\rho - \bar{\rho}(z)] dz}{\delta x} \quad ,$$

where $\bar{\rho}$ is a horizontally averaged density.

The errors associated with this scheme can be examined by carrying a forward integration for an unforced problem with quiescent initial conditions and an initial perturbation density $\rho - \bar{\rho}$ dependent only on z. The initial pressure gradient is zero up to truncation errors and its departure from zero acts as a spurious forcing. Figure 2 shows the bottom relief (upper left), the temperature (upper right), the zonal velocity (lower left) and the transport (lower right) after ten days of integration for a domain covering the Mid Atlantic Bight. Notice that the erroneous velocities are contained to within 0.056 cm/s. In this computation, the vertical interpolation was done with natural splines and the finite differencing of the gradient is of second order.

The algorithm for the pressure gradient has been tested for various combinations of vertical interpolation and horizontal difference schemes using the seamount test case of Beckmann and Haidvogel (1993). The geometrical parameters of the seamount, the background density and the initial density perturbation (independent of the horizontal coordinates) used here correspond to the test case from their paper with Burger number $S = 1.0$. The grid resolution was 4km and there were 14 σ levels. In figure 3, the seamount relief (bottom-right panel), the transport (bottom-left) and zonal and vertical velocity at tracer points (upper panels) are shown at day 10 after initialization. The maximum of the velocity over the model domain has an initial value of 0 cm/s and after 10 days remains below 0.02 cm/s.

Preparation of Bottom Relief

The close representation of the actual bottom relief in the model is limited by the horizontal grid resolution and computational considerations. The latter include the filtering of short scales in the bottom relief and the reduction of the ratio $\delta h/h$. Two filters, designed for these purposes and used to prepare the model bottom relief, are described below.

Weighted Median Filter

Error estimates of Deleersnijder & Beckers (1992) suggest that the short scales of the bottom relief are passed eventually to the fields. It is therefore desirable to filter the short scales from the gridded bottom relief. Readily available low pass filters can be used effectively for this purpose with acceptable distortion of the bottom relief if there are not steep gradients, e.g. shelf break or canyons. For the latter, a weighted median filter has been designed to remove specifically two grid point oscillations and yet able to retain the steep gradients. The filter is an extension of one dimensional filters proposed by Tukey (1977) and Mallows (1979).

The weighted median filter algorithm is as follows. Given a gridded field $h(i,j)$ and (i,j) an interior grid point an array $\mathbf{v}$ of length 16 is formed by inserting the center value, $h(i,j)$, four times; each of the edge points $h(i,j+1), h(i,j-1), h(i+1,j), h(i-1,j)$ twice and the corner points $h(i+1,j+1), h(i-1,j-1), h(i+1,j-1), h(i-1,j+1)$ once. The array $\mathbf{v}$ is then sorted by magnitude and the field at (i,j) is replaced by the average of the eighth and ninth components of the sorted array. At the SW grid corner point,

Figure 2.

Figure 3.

the array $\mathbf{v}$ has four components, namely $h(1,1), h(1,2), h(2,1), h(2,2)$ and the median of the array is the average of the second and third component of the sorted array. A similar construction is used for the other corners. For the edge points at the southern boundary, the array $\mathbf{v}$ has eight components, formed by taking the points $h(i,1), h(i,2)$ twice, and the points $h(i-1,1), h(i+1,1), h(i-1,2), h(i+1,2)$ once. The median is the average of the fourth and fifth components of the sorted array. A similar construction is done at the other edges. Convergence is usually achieved after tens of iterations.

Local Smoother

Extrapolation errors grow, as indicated above as, $\delta h/\delta z$; which, for a fixed σ-partition, scales as $r = \delta h/h$. Beckman and Haidvogel(1993) find a similar dependence on the error growth due to extrapolation for their schemes. It is desirable, then, to remove regions of high r, which normally occur in isolated regions. To this effect, given a bottom relief h_{target}, we seek the minimizer h_F of functional

$$J[h] = \int_V \left[\frac{1}{2} \nabla h \cdot \nabla h + hW \right] dV$$

among functions h that coincide with h_{target} at the boundary. Here

$$W = \begin{cases} \nabla^2 h_{target} & \text{if } \nabla h \cdot \nabla h \leq r_0^2 h^2 \\ 0 & \text{otherwise} \end{cases} .$$

The minimizer h_F of J satisfies

$$\nabla^2 h_F = \nabla^2 h_{target}.$$

in the domain for which $|\nabla h_F| < r_0 h_F$. Otherwise, for instance for steep or shallow slopes, h_F is locally harmonic. For the gridded functions, the Polak-Ribiere algorithm (Polak, 1971) is used to approximate a minimizer of the discretized functional.

The preparation of the bottom relief is illustrated for a region in the Mediterranean Sea that includes the Sicily Straits (figure 4). The upper left panel shows the topography from an extraction of NOAA-ETOPO5. The upper right panel shows the same topography after clipping depths which are less than 20 meters. The clipped topography after 61 iterations with the weighted median filter is shown in the lower left panel. Patches of high (~ 4) $\delta h/\delta z$ values are reduced to a maximum of ~ 1.5 using the local filter. The model topography shown in the lower right panel was obtained after final weighted median filter iterations.

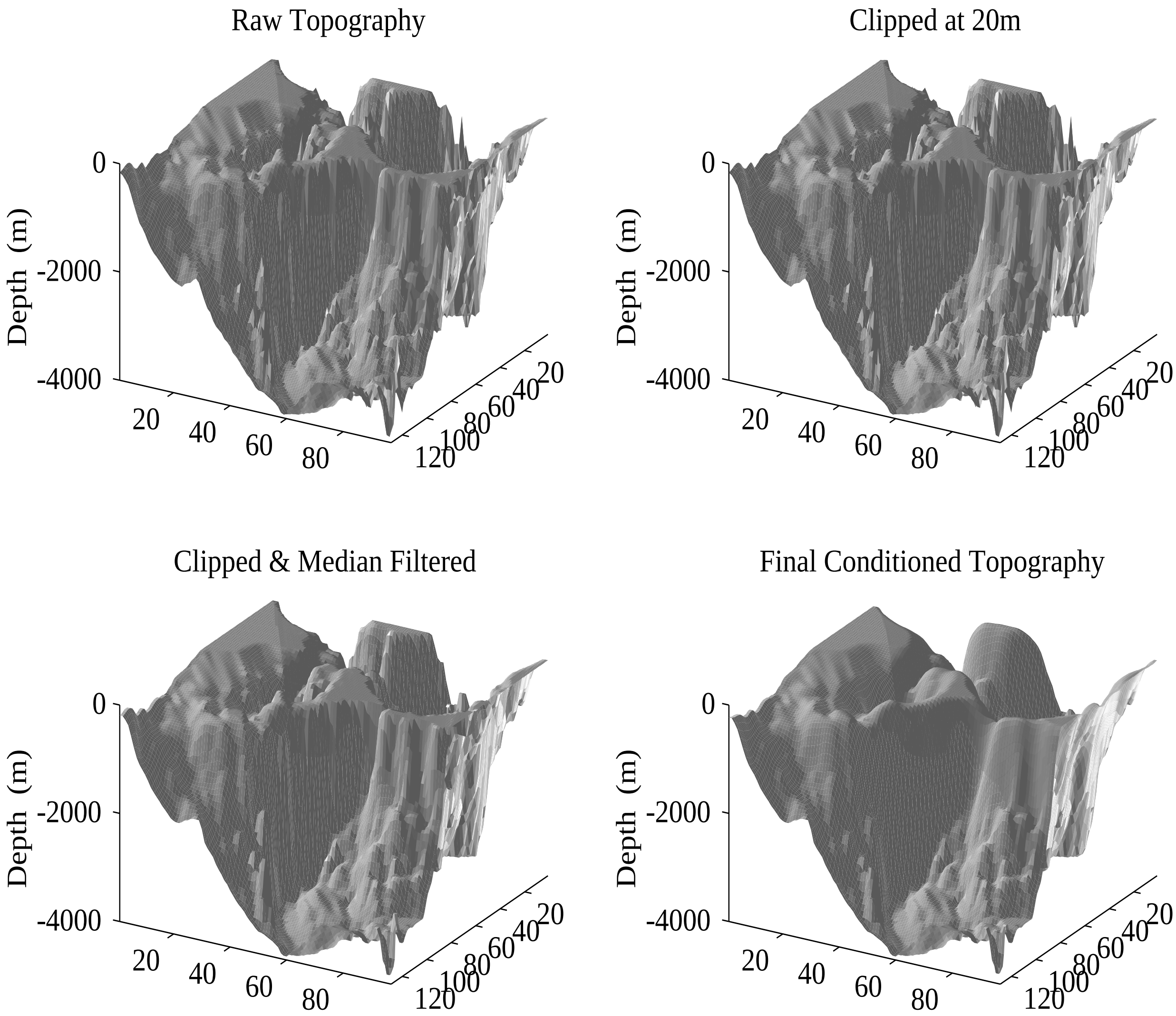

Figure 4. Topography in and around the Straits of Sicily in various stages of conditioning. All views are looking northwest with North Africa on the left, Italy on the right and Sardinia on the far edge. Upper left panel: raw topography. Upper right panel: topography with depths shallower than 20m reset to 20m. Lower left: results of previous panel with 61 iterations of the median filter. Lower right: results of previous panel with application of local smoother and clean up application of median filter.

Subgrid parameterization

Vertical mixing parameterization is based upon the K-profile parameterization (Troen and Mahrt, 1986) as developed and validated by Large, McWilliams and Doney (1994) for the ocean upper boundary layer. In the shelf interior, below the mixed layer, the parameterization of shear instability is in terms of a Richardson number (Pacanowski and Philander, 1981) and that of the internal waves is in terms of an additive constant vertical diffusivity coefficient. The bottom stress uses the wave-enhanced bottom roughness parameterization of Grant and Madsen (1982) as modified by Keen and Glenn (1993). Horizontal lateral diffusivity and mixing are taken to be constant. Parameter calibration is carried out using observations.

Model Software

The primitive equation model includes, in addition to the prognostic algorithms described above, a modular, intermittent, optimal interpolation package that allows the assimilation of gridded fields produced independently of the model by an optimal interpolation of all available data. Post-processing includes a program (PREEVA) to study averaged and detailed local vorticity and energy balances.

The primitive equation model software is an integral part of the GOES (Generic Oceanic Estimation System) system. Within the system the data preparation (quality control, data reduction and gridded representation), model run, data visualization and the analysis of model output is streamlined through the execution of mutually compatible modules allowing simple replacement of data filters and algorithms.

Simulations

Although model refinements continue, the model is routinely used for scientific research in a number of regions in the world's coastal oceans, including the Middle Atlantic Bight, Massachusetts Bay, Straits of Sicily, Gulf Stream separation at Cape Hatteras, and the Iceland Shelf / Iceland Faroes Front. An example of a regional simulation of the Middle Atlantic Bight is shown in figure 5. The topography, which varies from 10m at the coast to 4500m, has been smoothed with the median filter and the local smoother described above. The filtering is weak, and the resulting topography (figure 5), retains the features that are shown in figure 2, including a steep shelfbreak. The model was initialized with a feature model for the Gulf Stream ring and meander region. Hydrographic data on the shelf was assimilated on the first day of the simulation, using an optimal interpolation

Figure 5.

data-assimilation technique. After 3 days, the model begins pinching off a Gulf Stream warm core ring, while eddies form in the shelfbreak front south of New England.

References

Beckmann, A. & Haidvogel, D. B. (1993) Numerical simulation of flow around a tall isolated seamount. Part I: Problem formulation and model accuracy, J. Phys. Ocean., 23, 1736-1753.

Bleck, R. (1978) Finite Difference Equations in Generalized Vertical Coordinates. Part I: Total Energy Conservation., Beiträge zur Physik der Atmosphäre, 51,360-372.

Bryan, K. (1969) A Numerical Method for the Study of the Circulation of the World Ocean. J. of Comp. Phys., 4 ,347-376.

Cox, M. D. (1984) A Primitive Equation, 3-Dimensional Model of the Ocean. GFDL Ocean Group Technical Report 1, Princeton NJ.

Deleersnijder, E. & Beckers, J. M. (1992) On the use of the σ-coordinate system in regions of large bathymetric variations, J. Marine Sys., 3, 381-390.

Grant, W. D. and O. S. Madsen (1982) Combined Wave and Current Interaction with a Rough Bottom. J. Geophys. Res., 92 ,8244-8264.

Haney, R. L. (1991) On the pressure gradient force over steep topography in sigma coordinate ocean models, J. Phys. Oceanog., 21, 610-619.

Keen, R. K. and S. Glenn (1994) A coupled Hydrodynamic-Bottom Boundary Layer Model of Ekman Flow on Stratified Continental Shelves. Unpublished Manuscript.

Large, W. G. , J. C. McWilliams and S. C. Doney (1994) An oceanic Vertical Mixing Scheme with a K-profile Boundary Layer Parametrization, Technical Report NCAR 070/93 11, Boulder Co.

LeBlond, P. H. , and L. A. Mysak (1978) Waves in the Ocean, Elsevier, New York, 602 pp.

Mallows, C. L. (1979) Some Theoretical Results on Tukey's 3R Smoother. In Smoothing Techniques for Curve Estimation. Gasser T. and M. Rosenblatt Eds. Springer-Verlag; (pp. 77-90).

McCalpin, J. D. (1994) A comparison of second-order and fourth-order pressure gradient algorithms in a σ-coordinate ocean model, J. Num. Meth. Fluids, 18, 361-383.

Miller, R. N., Robinson, A. R. & Haidvogel, D. B. (1983) A Baroclinic Quasigeostrophic Open Ocean Model. J. Comp. Phys., 50, 38-70.

Milliff, R. F. (1990) A Modified Capacitance Matrix Method to Implement Coastal Boundaries in the Harvard Open Ocean Model. Math. and Comp. Sim., 31, 541-564.

Özsoy, E., Lozano, C. J. & Robinson, A. R. (1992) A Consistent Baroclinic Quasigeostrophic Ocean Model in Multiply Connected Ocean Domains. Math. and Comp. Sim., 34(1), 51-79.

Pacanowski, R. C. and S. G. H. Philander (1981) Parameterization of vertical mixing in numerical models of tropical oceans. J. Phys. Oceanogr.,11 ,1443-1451.

Pedlosky, J. (1987) Geophysical Fluid Dynamics. $2^{nd}ed.$ Springer-Verlag, New York.

Polak, E. (1971) Computational Methods in Optimization. Academic Press, New York.

Spall, M. A. (1988) Regional Ocean Modelling: Primitive Equation and Quasigeostrophic Studies. Harvard Ocean Model Report, 28, Reports in Meteorology and Oceanography, Harvard University, Cambridge MA, 282 pages.

Spall, M. A. & Robinson, A. R. (1989) A new open ocean, hybrid coordinate primitive equation model. Math. and Comp. in Sim., 31, 241-269.

Serrin, J. (1959) Mathematical Principles of Classical Fluid Mechanics in Handbuk Der Physik, 8/1 Fluid Dynamics I, Flügge, S. and C. Truesdell Eds. Springer-Verlag, Berlin.

Simmons A. J. and D. M. Burridge (1981) An energy and Angular Momentum Conserving Vertical Finite Difference Scheme and Hybrid Vertical Coordinates., Monthly Weather Rev., 109,758-766.

Troen, I.B. and L. Mahrt (1986) A simple model of the atmospheric boundary layer; sensitivity to surface evaporation. Boundary Layer Meteor., 37, 129-148.

Tukey, J. W. (1977) Exploratory Data Analysis. Addison-Wesley, Reading MA.

Walstad, L. J. & Robinson, A. R. (1993) A Coupled Surface Boundary Layer - Quasigeostrophic Ocean Model. Dyn. Atmos. and Oceans, 18, 151-207.